Title: Magnetoelectric Effect in Ceramics Based on Bismuth Ferrite

Author: Elżbieta Jartych, Tomasz Pikula, Karol Kowal, Jolanta Dzik, Piotr Guzdek, Dionizy Czekaj

Citation style: Elżbieta Jartych, Tomasz Pikula, Karol Kowal, Jolanta Dzik, Piotr Guzdek, Dionizy Czekaj. (2016). Magnetoelectric Effect in Ceramics Based on Bismuth Ferrite. "Nanoscale Research Letters" (2016, no. 1, s. 1-8), doi 10.1186/s11671-016-1436-3

Jartych et al. Nanoscale Research Letters (2016) 11:234
DOI 10.1186/s11671-016-1436-3

Nanoscale Research Letters

NANO EXPRESS Open Access

Magnetoelectric Effect in Ceramics Based on Bismuth Ferrite

Elżbieta Jartych[1*], Tomasz Pikula[1], Karol Kowal[1], Jolanta Dzik[2], Piotr Guzdek[3] and Dionizy Czekaj[2]

Abstract

Solid-state sintering method was used to prepare ceramic materials based on bismuth ferrite, i.e., $(BiFeO_3)_{1-x}$–$(BaTiO_3)_x$ and $Bi_{1-x}Nd_xFeO_3$ solid solutions and the Aurivillius $Bi_5Ti_3FeO_{15}$ compound. The structure of the materials was examined using X-ray diffraction, and the Rietveld method was applied to phase analysis and structure refinement. Magnetoelectric coupling was registered in all the materials using dynamic lock-in technique. The highest value of magnetoelectric coupling coefficient α_{ME} was obtained for the $Bi_5Ti_3FeO_{15}$ compound ($\alpha_{ME} \sim 10$ mVcm^{-1} Oe^{-1}). In the case of $(BiFeO_3)_{1-x}$–$(BaTiO_3)_x$ and $Bi_{1-x}Nd_xFeO_3$ solid solutions, the maximum α_{ME} is of the order of 1 and 2.7 mVcm^{-1} Oe^{-1}, respectively. The magnitude of magnetoelectric coupling is accompanied with structural transformation in the studied solid solutions. The relatively high magnetoelectric effect in the Aurivillius $Bi_5Ti_3FeO_{15}$ compound is surprising, especially since the material is paramagnetic at room temperature. When the materials were subjected to a preliminary electrical poling, the magnitude of the magnetoelectric coupling increased 2–3 times.

Keywords: Multiferroics, Ceramic materials, Bismuth ferrite, Aurivillius compounds, Magnetoelectric effect

Background

Multiferroics are the class of intelligent materials which exhibit at least two from the three possible *ferro-* orders, i.e., ferromagnetic (also ferrimagnetic, antiferromagnetic, or ferrotoroidal), ferroelectric, and ferroelastic [1, 2]. Especially interesting from the application point of view is the group of magnetoelectrics which offers long-range ordering of the elementary magnetic moments as well as long-range ordering of the electric dipoles [3, 4]. Moreover, they exhibit a coupling between the magnetic and the electric sub-systems what makes possible induction of magnetization by applying an external electric field or induction of electric polarization by applying an external magnetic field [5, 6]. Therefore, the so-called magnetoelectric (ME) effect attracts a lot of interest also from the basic research point of view. Experimentally, ME effect is measured and expressed by magnetoelectric coupling coefficient, α_{ME}, typically specified in units of mVcm^{-1} Oe^{-1}.

Although the magnetoelectric effect is known since the 1960s of the last century, an intensive growth of interest in the possibilities of practical application of this phenomenon occurred in the late 1990s. In 2003 and 2004, the first results confirming the possibility of switching electrical polarization by an external magnetic field in $TbMnO_3$ and $TbMn_2O_5$ were published [7, 8]. Although this effect has been observed only at low temperatures, these works gave rise to many new research projects focusing on the α_{ME} optimization. The higher value of this parameter can be achieved in magnetoelectric material at room temperature, and the wider range of its potential applications can be expected. The most frequently mentioned prototypes of magnetoelectric devices which were developed so far are magnetic field sensors [9–11] and energy harvesting devices [12–14]. Among the new proposals for the use of magnetoelectric coupling phenomenon, the most spectacular and forward-looking ideas seem to be new-generation memories [15–17], spintronic devices (e.g., spin valves, magnetic tunnel junctions) [18–20], microwave, millimeter-wave devices and miniature antennas [14], and wireless medical tools (e.g., for endoscopy and brain imaging) [14]. The implementation of such innovative devices requires, however, the elaboration of materials having possibly high magnetoelectric coupling coefficient.

* Correspondence: e.jartych@pollub.pl
[1]Institute of Electronics and Information Technology, Lublin University of Technology, Nadbystrzycka 38a Str., 20-618 Lublin, Poland
Full list of author information is available at the end of the article

The magnetoelectric effect is especially high in composite materials. In particulate composites, like $BaTiO_3/CoFe_2O_4$, $PbZr_{1-x}Ti_xO_3$(PZT)/$Tb_{1-x}Dy_xFe_2$(Terfenol-D), and $Ba_{0.8}Pb_{0.2}TiO_3/CuFe_{1.8}Cr_{0.2}O_4$, the value of α_{ME} is of the order of 100–130 $mVcm^{-1}$ Oe^{-1} [6]. The laminated composites exhibit the largest value of α_{ME}, e.g., in PZT/Terfenol-D laminates, ME response achieves ~ 4.7 Vcm^{-1} Oe^{-1} [21] or even 90 Vcm^{-1} Oe^{-1} in laminated PZT/Permendur composites [22]. The magnetoelectric coupling is also observed in nanostructured multiferroic ceramic materials (e.g., $YMnO_3$ [23]), semiconducting membranes galvanically filled with a magnetostrictive material (e.g., InP membrane filled with Ni [24]) as well as in nanocomposite thin films (e.g., $CoFe_2O_4$ polymer nanocomposite thin films [25]).

The synthesis of new, single-phase, multiferroic materials which exhibit high value of the magnetoelectric coupling coefficient is still a challenge. Until now, the best recognized single-phase multiferroic compound is bismuth ferrite $BiFeO_3$ in which the ferroelectric and antiferromagnetic ordering coexist at ambient temperature (antiferromagnetic Néel temperature $T_N = 643$ K, ferroelectric Curie temperature $T_C = 1100$ K) [26]. However, due to the cycloidal modulation of spin arrangement, the linear magnetoelectric effect in bismuth ferrite in the form of bulk polycrystalline sample is not observed. In thin films of $BiFeO_3$, where spin cycloid disappears, a giant magnetoelectric coupling was observed, $\alpha_{ME} \sim 3$ Vcm^{-1} Oe^{-1}, as reported in [27]. Therefore, many current investigations tend to destroy the spin cycloid and to release the inherent magnetization in order to improve multiferroic properties of $BiFeO_3$. This may be achieved, e.g., by structural modifications or deformations introduced by cation substitution or doping or creating of solid solutions of $BiFeO_3$ with other materials with ABO_3 type of structure.

In the present work, three types of ceramic materials based on bismuth ferrite $BiFeO_3$ were prepared by solid-state sintering method, i.e., $(BiFeO_3)_{1-x}$–$(BaTiO_3)_x$ solid solutions, bismuth ferrite doped by neodymium $Bi_{1-x}Nd_xFeO_3$, and the Aurivillius $Bi_5Ti_3FeO_{15}$ compound. The structure and selected magnetic and electric properties of these materials have been already investigated and reported [28–32]. However, one can note that there is lack of data of direct measurements of magnetoelectric coupling in materials based on the bismuth ferrite. Dynamic lock-in technique was adopted in the present study to measure the magnetoelectric coupling effect. In contrast to static and quasi-static methods, the dynamic technique allows avoiding errors caused by charge accumulation on the grain boundaries in polycrystalline samples [6, 33]. The value of the magnetoelectric coupling coefficient was determined using formula

$$\alpha_{ME} = \frac{dE}{dH_{DC}} = \frac{1}{t}\,\frac{V_{OUT}}{H_{AC}}, \tag{1}$$

where V_{OUT} is the output voltage (induced between the sample surfaces due to the magnetoelectric effect) registered by the lock-in amplifier, t is the thickness of the sample (in the form of disk), H_{DC} is the magnitude of the DC magnetic field produced by an electromagnet, and H_{AC} is the amplitude of the small sinusoidal magnetic field superimposed onto the DC magnetic field [6, 33].

The aim of our studies was to compare the magnitude of magnetoelectric coupling in ceramic materials mentioned above and to determine the influence of the structure on the value of magnetoelectric response of a given material.

Methods

The conventional solid-state sintering method was used to prepare the samples from the oxides and commercial compounds of 99.9 % purity. In the case of $(BiFeO_3)_{1-x}$–$(BaTiO_3)_x$ solid solutions, the synthesis was performed according to the following reaction:

$$\begin{aligned}&(Bi_2O_3)_{\frac{1-x}{2}} + (Fe_2O_3)_{\frac{1-x}{2}} + (TiO_2)_x \\ &\quad + (BaCO_3)_x \rightarrow (BiFeO_3)_{1-x}\text{–}(BaTiO_3)_x \\ &\quad + (CO_2)_x.\end{aligned} \tag{2}$$

As recently reported, $(BiFeO_3)_{1-x}$–$(BaTiO_3)_x$ solid solutions exhibit maximum magnetoelectric coupling within a narrow composition range, i.e., $x = 0.2$–0.3 which is connected with the structural transformation of the samples from rhombohedral to cubic symmetry [34]. As reported in our earlier work [35], the magnetoelectric properties of $(BiFeO_3)_{1-x}$–$(BaTiO_3)_x$ solid solutions are strongly dependent on the sintering temperature T and the highest magnetoelectric effect was observed for the sample with $x = 0.3$ sintered at $T = 1153$ K. Therefore, in current studies after the preliminary synthesis at 1123 K for 2 h, the sintering was performed at temperature $T = 1153$ K for 4 h. After that, the ceramics were annealed in air at a temperature of 823 K for 10 h and then cooled with a linear decrease in temperature (100 K h^{-1}). Three samples with the barium titanate concentration $x = 0.25$, 0.4, and 0.5 were prepared in the form of disks with a diameter of 10 mm and 1-mm thickness. The concentrations of $x = 0.25$, 0.4, and 0.5 were selected in order to check whether there was a structural transformation in this range and for which barium titanate contents the maximum magnetoelectric coupling might be observed.

The second series of the samples, i.e., $Bi_{1-x}Nd_xFeO_3$ solid solutions, was prepared by doping bismuth ferrite by neodymium ions according to the reaction

$$(1-x)Bi_2O_3 + xNd_2O_3 + Fe_2O_3 \rightarrow 2Bi_{1-x}Nd_xFeO_3. \quad (3)$$

The ceramic disks with 10-mm diameter and 2-mm thickness were obtained after calcination at 1023 K for 10 h and sintering in air at a temperature of 1273 K for 24 h. The detailed information about the fabrication process has been published elsewhere in [36, 37].

The synthesis of bismuth ferrite $BiFeO_3$ with ferroelectric bismuth titanate $Bi_4Ti_3O_{12}$ leads to obtaining the Aurivillius $Bi_5Ti_3FeO_{15}$ compound. High-purity oxide powders were mixed according to the reaction

$$5Bi_2O_3 + 6TiO_2 + Fe_2O_3 \rightarrow 2Bi_5Ti_3FeO_{15}. \quad (4)$$

The preliminary synthesis of the compound was carried out in air at 1023 K for 10 h while the sintering was performed in air at a temperature of 1253 K for 3 h. The detailed information about the preparation process has been published in our earlier works [38, 39].

The crystalline structure of the sintered samples was investigated by X-ray diffraction (XRD) using the Philips PW3710 diffractometer with CoKα radiation or PANalytical Empyrean diffractometer using CuKα radiation. The phase and structural analysis of the recorded XRD patterns was performed with an X'Pert High Score Plus computer program equipped with the ICDD PDF data base and Rietveld method of the crystalline structure refinement.

Investigations of the magnetoelectric properties have been performed by the dynamic lock-in technique. The samples were placed in a time-varying DC magnetic field created by an electromagnet and controlled by a programmable DC power source (Fig. 1).

The DC field was modulated by a small sinusoidal AC magnetic field produced by the Helmholtz coils. The voltage induced between the sample surfaces due to the magnetoelectric effect (ME signal) was transmitted to the lock-in amplifier. The amplifier is a key element of the system since it measures and transmits to the computer only this part of the ME signal which is in-phase with the AC modulation field of frequency f. Thus, the output signal (V_{OUT}) measured as a function of the DC field intensity (H_{DC}) gives an information about the ME effect at a low-AC magnetic field but for different working points of the magnetostrictive samples [33]. The measurements of the α_{ME} coefficient were performed by recording V_{OUT} under the applied DC magnetic field of the magnitude H_{DC} varying within the range of values from 0.1 to 4.5 kOe, while the amplitude H_{AC} was constant during the experiment and it was equal to 5 Oe (which is significantly lower than H_{DC}). The frequency f of the AC modulation field was equal to 1 kHz. In the case of $(BiFeO_3)_{1-x}$–$(BaTiO_3)_x$ solid solutions and the Aurivillius $Bi_5Ti_3FeO_{15}$ compound, each sample was measured two times, before and after additional electrical poling, in order to verify how the initial polarization of the

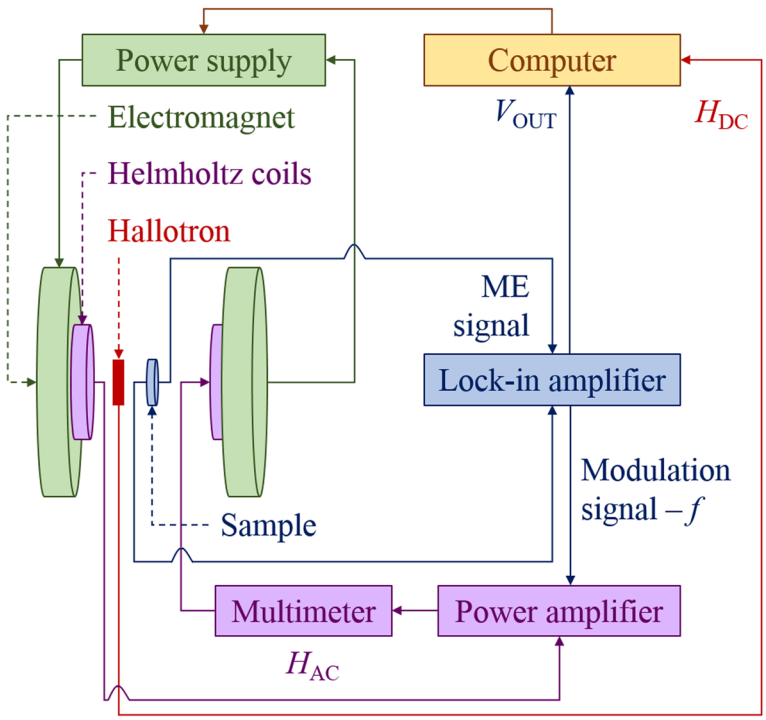

Fig. 1 The experimental setup for the dynamic measurement of the magnetoelectric effect [33]

material affects its magnetoelectric properties. Poling was a process, in which a strong electric field (~3 kV mm^{-1}) was applied across the sample at the increased temperature through 1 h before the measurement leading to align the randomly oriented dipoles into one direction. As proved in our earlier work [35], the parallel orientation of the applied electric field versus the magnetic one is better to maximize the value of the α_{ME} coefficient. In the case of $Bi_{1-x}Nd_xFeO_3$ solid solutions, the measurements of α_{ME} as a function of H_{DC} were performed without initial electrical poling. Moreover, for all the samples, the frequency characteristics were collected in the range of 100 Hz–10 kHz. The measurable magnetoelectric effect was registered above 100 Hz. In the range of 100 Hz–1 kHz, the ME coupling increased rapidly and then stabilized above 1 kHz. Due to the inductance of the Helmholtz coils, the frequency range was limited up to 10 kHz. The kHz range of frequency is justified in the context of possible applications, mainly in energy harvesting devices.

Results and Discussion

Results of X-ray Diffraction Studies

The results of X-ray diffraction studies for $Bi_{1-x}Nd_xFeO_3$ solid solutions and the Aurivillius $Bi_5Ti_3FeO_{15}$ compound have been published in our previous works [37–39]. It was found that with an increase of Nd content in $Bi_{1-x}Nd_xFeO_3$ solid solutions, within the range of $x = 0.2$–0.3, a structural phase transition from rhombohedral to orthorhombic system occurs. The obtained solid solutions were pure and homogeneous samples with very low concentration of secondary phases or without any impurities [37]. In the case of the $Bi_5Ti_3FeO_{15}$ compound, a pure Aurivillius phase with orthorhombic lattice (*Fmm2* no. 42 space group) was obtained [38, 39].

Figure 2 presents the results of XRD measurements performed in the current work for $(BiFeO_3)_{1-x}$–$(BaTiO_3)_x$ solid solutions.

The results of the Rietveld refinement method allowed us to conclude that all the obtained samples are no single-phase materials, namely, for $x = 0.25$, the diffractograms revealed two phases, i.e., rhombohedral *R3c* (75 %) and tetragonal *P4mm* (25 %) one. Unfortunately, due to the intensive signal from the sample holder, this estimation of the relative contribution of the phases is uncertain. In the case of $x = 0.4$, three phases were recognized, namely, rhombohedral *R3c* (51 %), cubic *Pm3m* (42 %), and tetragonal *P4mm* (7 %). Finally, XRD pattern for the sample with $x = 0.5$ revealed two phases, i.e., rhombohedral (51 %) and tetragonal (49 %). The obtained result is not fully consistent with the literature data. As reported in [40, 41], the crystallographic symmetry of $(BiFeO_3)_{1-x}$–$(BaTiO_3)_x$ solid solutions changes from rhombohedral for $0 < x < 0.3$ to cubic for $0.3 < x < 0.93$ and, finally, to tetragonal for $x > 0.93$. The structural transformation in sintered $(BiFeO_3)_{1-x}$–$(BaTiO_3)_x$ solid solutions from rhombohedral to cubic has been observed by us for the $BaTiO_3$ concentration $x = 0.3$ [42]. However, in the case of the analogous solid solutions prepared by us using the mechanical activation method and subsequent isothermal annealing [43], the structural transformation from rhombohedral to cubic symmetry occurred within the region of $x = 0.4$–0.7. Similarly, such gradual transformation was observed for $(BiFeO_3)_{1-x}$–$(SrTiO_3)_x$ solid solutions in Ref. [44], where the structural transformation proceeded for $x = 0.5$–0.7 with the multiphase region in between.

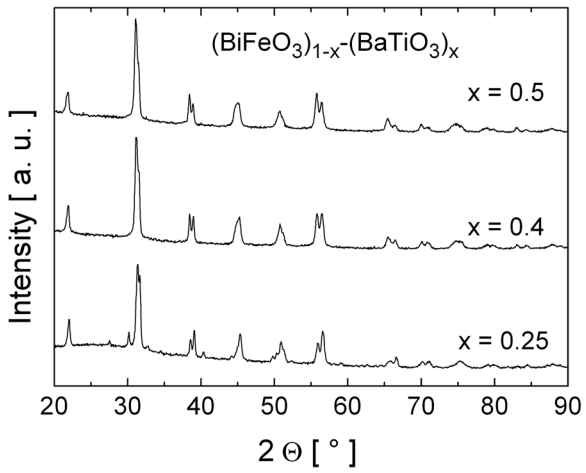

Fig. 2 XRD patterns for $(BiFeO_3)_{1-x}$–$(BaTiO_3)_x$ solid solutions with barium titanate concentration $x = 0.25$, 0.4, and 0.5. Low intensity peaks observed for $x = 0.25$ are from the sample holder

Magnetoelectric Effect in $(BiFeO_3)_{1-x}$–$(BaTiO_3)_x$ Solid Solutions

The measurements of α_{ME} as a function of H_{DC} were performed for the set of $(BiFeO_3)_{1-x}$–$(BaTiO_3)_x$ samples with different x values. Figure 3 presents the results for $x = 0.4$ as an example.

For all the investigated samples, the curves $\alpha_{ME}(H_{DC})$ do not retrace the same path on the reversal magnetic field when the AC field parameters were fixed. The hysteresis is repeatable (as seen in Fig. 3) and may be connected with the change of orientation of magnetic domains. These results are in consistence with our previous works [35, 42]. Also, the fact that the values of the α_{ME} coefficient are generally higher for the samples which were initially polarized electrically has been confirmed. Figure 4 shows the α_{ME} dependency on the modulation frequency assuming a constant value of $H_{DC} = 600$ Oe.

The experiment showed that the frequency dependence of the α_{ME} coefficient exhibits a strong variability

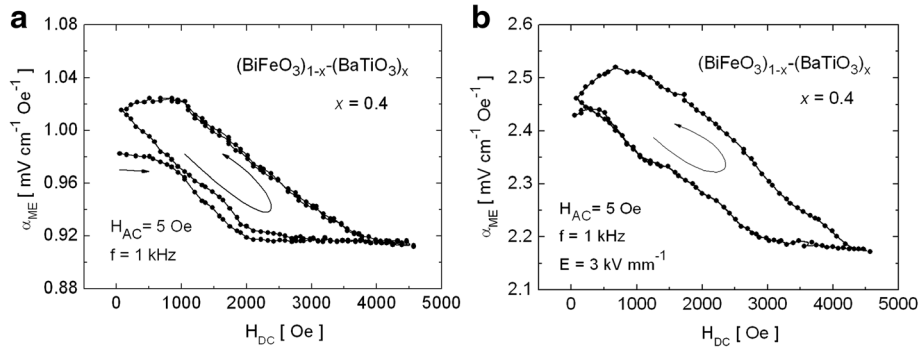

Fig. 3 Variation of α_{ME} with H_{DC} for the $(BiFeO_3)_{1-x}$–$(BaTiO_3)_x$ samples with $x = 0.4$: **a** before electrical poling and **b** after electrical poling at 368 K

for $f < 2$ kHz. This effect can be caused by the discharge of electric charges accumulated on the surfaces of the investigated samples due to the resistance of the materials [33]. Above the threshold of $f = 2$ kHz, the characteristics are almost flat for all the samples. The flat characteristic is preferred for the practical applications because it allows for a stable operation of the magnetoelectric device in a wide range of frequency. Thus, $f = 2$ kHz would be the optimum frequency for application of the investigated $(BiFeO_3)_{1-x}$–$(BaTiO_3)_x$ solid solutions, for example, as the AC magnetic field sensors.

The dependence of the α_{ME} coefficient on the concentration of barium titanate is presented in Fig. 5 (the maximum values from the frequency dependencies of α_{ME}).

The maximum value of $\alpha_{ME} = 2.84$ mVcm^{-1} Oe^{-1} achieved in this study for the electrically poled sample with $x = 0.4$ is higher even up to 85 % when compared with the previous results for the sample with $x = 0.3$ ($\alpha_{ME} = 1.53$ mVcm^{-1} Oe^{-1}) [35] and about three times higher than the results reported by Yang for $0.75BiFeO_3$–$0.25BaTiO_3$ ($\alpha_{ME} = 0.87$ mVcm^{-1} Oe^{-1}) [34]. It may be seen that the value of the α_{ME} coefficient first increases with an increase of x which is connected with suppression of the cycloidal spin structure in $BiFeO_3$. For $x = 0.2$–0.4, the magnitude of magnetoelectric coupling is practically constant and then decreases. Electrical poling allows increasing the value of α_{ME} by 2–3 times what may be caused with the presence of the tetragonal phase. It may be supposed that multiphase structure of $(BiFeO_3)_{1-x}$–$(BaTiO_3)_x$ solid solutions for $x = 0.25$–0.5 promotes greater magnetoelectric coupling, especially after initial electrical poling of the samples.

Magnetoelectric Effect in $Bi_{1-x}Nd_xFeO_3$ Solid Solutions

In the case of $Bi_{1-x}Nd_xFeO_3$ solid solutions, α_{ME} reaches the maximum value for 1 kOe and then quickly drops. Figure 6 presents the curves $\alpha_{ME}(H_{DC})$ for $x = 0.2$ and 0.4 as an example. It was observed that weak hysteresis in $\alpha_{ME}(H_{DC})$ dependence occurred in the range of neodymium concentration $x = 0.1$–0.3, while for $x \geq 0.4$, the hysteresis disappeared.

The frequency dependence of the α_{ME} coefficient for $Bi_{1-x}Nd_xFeO_3$ solid solutions is presented in Fig. 7 for various x. The dependence shows similar behavior as for $(BiFeO_3)_{1-x}$–$(BaTiO_3)_x$ solid solutions, the α_{ME} coefficient reaches maximum for 1–2 kHz and then saturates.

It may be seen that α_{ME} initially increases with an increase of x and reaches the maximum value $\alpha_{ME} \sim 2.7$ mVcm^{-1} Oe^{-1} for $x = 0.2$. This increase is attributed

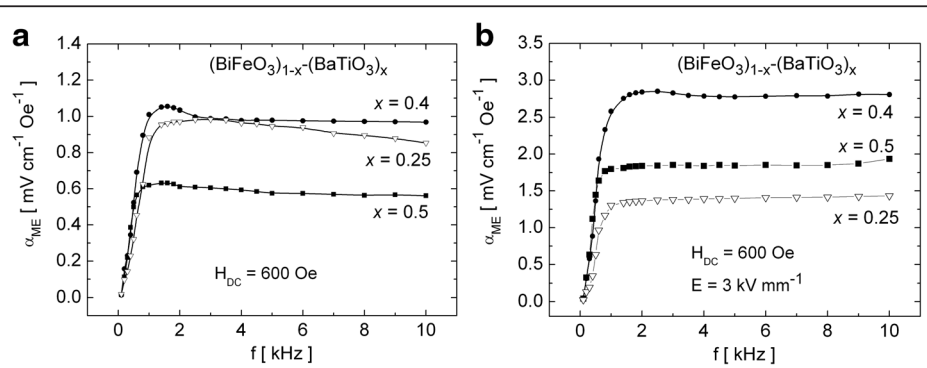

Fig. 4 The frequency dependence of the α_{ME} coefficient for the $(BiFeO_3)_{1-x}$–$(BaTiO_3)_x$ samples with $x = 0.25$, 0.4, and 0.5: **a** before electrical poling and **b** after electrical poling at 368 K

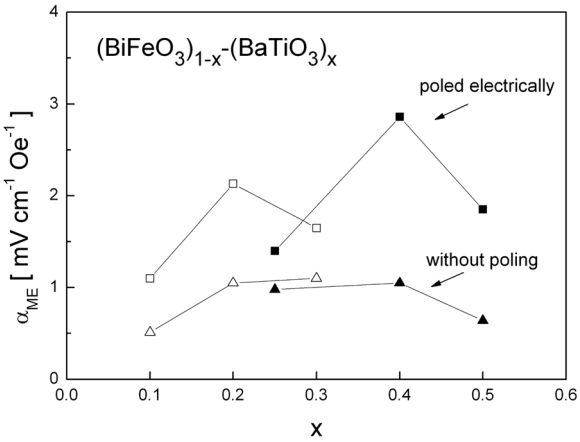

Fig. 5 The composition dependence of the α_{ME} coefficient for the $(BiFeO_3)_{1-x}$–$(BaTiO_3)_x$ samples; *open symbols*—data from our works [35, 48], *filled symbols*—results in this work

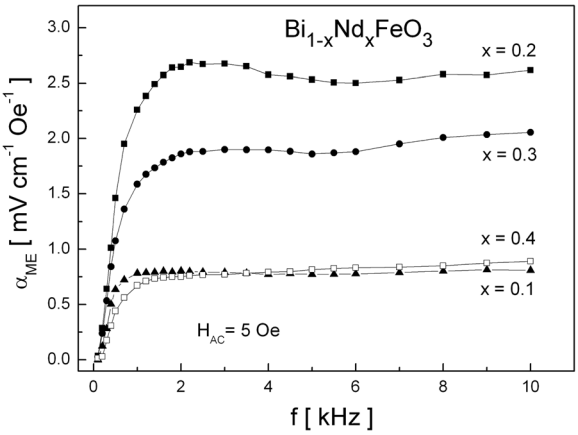

Fig. 7 The frequency dependence of the α_{ME} coefficient for $Bi_{1-x}Nd_xFeO_3$ solid solutions with $x = 0.1$–0.4

to quenching of the cycloidal spin structure of $BiFeO_3$. Further increase of x causes monotonical decrease of α_{ME}, and for $x = 0.7$–0.9, the ME signal was unmeasurably small. The changes of magnetoelectric coupling coefficient in $Bi_{1-x}Nd_xFeO_3$ solid solutions are accompanied with structural transformation from rhombohedral to orthorhombic system for $x = 0.2$–0.3.

Magnetoelectric Effect in the Aurivillius $Bi_5Ti_3FeO_{15}$ Compound

As proved by XRD, Mössbauer spectroscopy, and magnetic measurements, the $Bi_5Ti_3FeO_{15}$ Aurivillius compound is a single-phase paramagnetic material within the broad temperature range 2–350 K (our earlier articles [38, 39, 45]). Despite being paramagnetic at room temperature, i.e., in the absence of magnetic long-range order, the sample shows magnetoelectric coupling (Fig. 8). Measurements show that the α_{ME} coefficient decreases almost linearly with an increase of H_{DC} and no hysteretic behavior was observed (Fig. 8a). The dependence of the α_{ME} on f shows an increase of the magnitude of ME response of the sample within relatively broad range of frequency 0–5 kHz (Fig. 8b). Above the threshold of $f = 5$ kHz, the characteristics are almost flat. As seen in Fig. 8, electrical poling allowed us to double the value of α_{ME}.

As shown in the latest theoretical first-principles calculations, for the four-layer Aurivillius-phase $Bi_5Ti_3FeO_{15}$ [46], there is a strong antiferromagnetic coupling between Fe^{3+} cations in the nearest-neighbor positions, characteristic of the superexchange interaction between

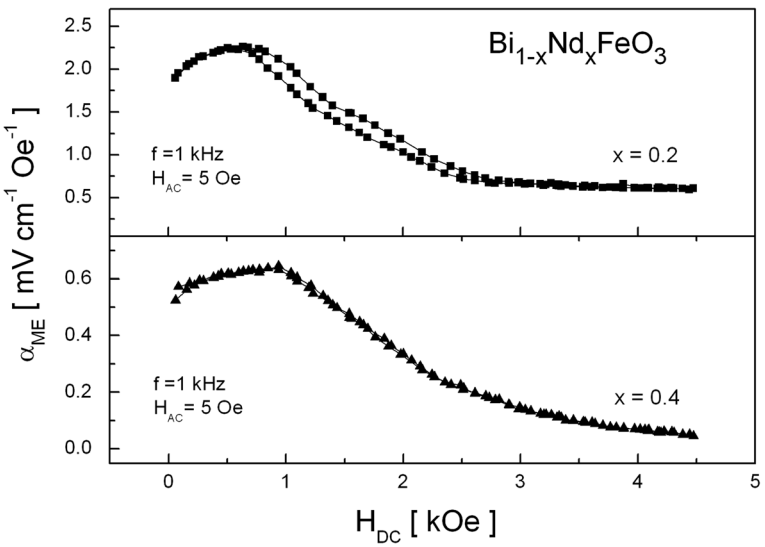

Fig. 6 Variation of α_{ME} with H_{DC} for $Bi_{1-x}Nd_xFeO_3$ solid solutions with $x = 0.2$ and $x = 0.4$

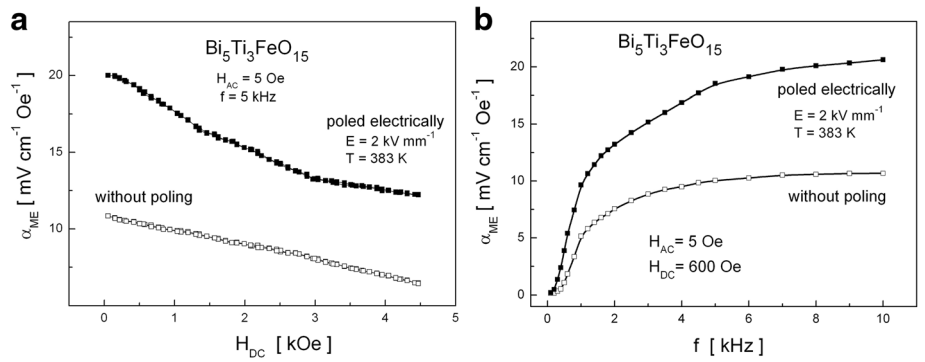

Fig. 8 a Variation of α_{ME} with H_{DC} and **b** frequency dependence of the α_{ME} coefficient for the $Bi_5Ti_3FeO_{15}$ compound without and with electrical poling

d^5 cations (Fe-O-Fe). Moreover, the coupling between further neighbors is rather weak and becomes negligible beyond second neighbors. Due to the relatively low concentration of magnetic cations in $Bi_5FeTi_3O_{15}$ and the short range of the magnetic superexchange interaction, it is unclear whether magnetic long-range order can occur in this system. Unexpectedly, our research shows that the magnetoelectric coupling in the $Bi_5Ti_3FeO_{15}$ compound is relatively high. We suppose that the ME coupling in this single-phase material may be connected with short-range magnetic ordering of Fe-rich nanoregions, which mimic $BiFeO_3$. Similar interpretation was reported for $Bi_5Ti_3FeO_{15}$ thin films grown by pulsed layer deposition with a robust magnetoelectric coupling of 400 mVcm^{-1} Oe^{-1} [47].

Conclusions

On the basis of the performed studies, it may be stated that the best candidate for the single-phase room-temperature multiferroic material is the Aurivillius $Bi_5FeTi_3O_{15}$ compound. Using solid-state sintering method, a pure single phase was successfully obtained. The ME effect in the $Bi_5FeTi_3O_{15}$ compound is present despite the absence of long-range magnetic order, and relatively strong ME signal cannot be caused by tiny inclusions of other phases. The existence of the magnetoelectric coupling in the paramagnetic Aurivillius $Bi_5FeTi_3O_{15}$ compound and explanation of mechanism of this coupling is open for future studies.

In the case of $(BiFeO_3)_{1-x}$–$(BaTiO_3)_x$ and $Bi_{1-x}Nd_xFeO_3$ solid solutions, the ME effect is connected with suppression of the cycloidal spin structure of $BiFeO_3$. The magnitude of magnetoelectric coupling depends on the concentration of barium titanate and neodymium in the bismuth ferrite structure. The maximum values of the magnetoelectric coupling coefficient were obtained for the compositions within the region of structural transformations.

As it was shown, an initial electrical poling allows increasing the ME effect 2–3 times. The frequency dependencies of α_{ME} have similar shapes for all the investigated materials and allowed us to determine the optimum frequency range, i.e., $f \geq 2$ kHz for $(BiFeO_3)_{1-x}$–$(BaTiO_3)_x$ and $Bi_{1-x}Nd_xFeO_3$ solid solutions and $f \geq 5$ kHz for the Aurivillius $Bi_5FeTi_3O_{15}$ compound. Moreover, no hysteretic behavior was observed in $\alpha_{ME}(H_{DC})$ dependence in the case of single-phase materials.

Competing interests

The authors declare that they have no competing interests.

Authors' contributions

The work presented here was carried out in collaboration between all authors. EJ defined the research theme, discussed and interpreted results of experiments, and drafted the manuscript. TP and KK performed Mössbauer spectroscopy experiments and elaborated spectra. JD and DC carried out XRD measurements and elaborated diffraction patterns. PG performed measurements of magnetoelectric coefficient. TP and KK helped EJ to complete the work. All authors read and approved the final manuscript.

Acknowledgements

The authors are very grateful to Dr. Katarzyna Osińska from the Institute of Technology and Mechatronics, University of Silesia, Poland, for the preparation of the samples.

Author details

[1]Institute of Electronics and Information Technology, Lublin University of Technology, Nadbystrzycka 38a Str., 20-618 Lublin, Poland. [2]Institute of Technology and Mechatronics, University of Silesia, Żytnia 12 Str., 41-200 Sosnowiec, Poland. [3]Institute of Electron Technology, Cracow Division, Zabłocie 39 Str., 30-701 Kraków, Poland.

Received: 12 February 2016 Accepted: 14 April 2016
Published online: 30 April 2016

References

1. Spaldin NA, Fiebig M (2005) The renaissance of magnetoelectric multiferroics. Science 309:391
2. Spaldin NA, Cheong SW, Ramesh R (2010) Multiferroics: past, present, and future. Phys Today 63:38
3. Eerenstein W, Mathur ND, Scott JF (2006) Multiferroic and magnetoelectric materials. Nature 442:759
4. Khomskii DI (2006) Multiferroics: different ways to combine magnetism and ferroelectricity. J Magn Magn Mater 306:1
5. Fiebig M (2005) Revival of the magnetoelectric effect. J Phys D Appl Phys 38:R123

6. Rivera JP (2009) A short review of the magnetoelectric effect and related experimental techniques on single phase (multi-) ferroics. Eur Phys J B 71:299
7. Hur N, Park S, Sharma PA, Ahn JS, Guha S, Cheong S (2004) Electric polarization reversal and memory in a multiferroic material induced by magnetic fields. Nature 429:392
8. Kimura T, Goto T, Shintani H, Ishizaka K, Arima T, Tokura Y (2003) Magnetic control of ferroelectric polarization. Nature 426:55
9. Bichurin MI, Petrov VM, Petrov RV, Kiliba YV, Bukashev FI, Smirnov AY, Eliseev DN (2002) Magnetoelectric sensor of magnetic field. Ferroelectrics 280:199
10. Duc NH, Huong Giang DT (2008) Magnetic sensors based on piezoelectric magnetostrictive composites. J Alloy Compd 449:214
11. Huong Giang DT, Duc NH (2009) Magnetoelectric sensor for microtesla magnetic-fields based on $(Fe_{80}Co_{20})_{78}Si_{12}B_{10}$/PZT laminates. Sensor Actuat A-Phys 149:229
12. Dong S, Zhai J, Li JF, Viehland D, Priya S (2008) Multimodal system for harvesting magnetic and mechanical energy. Appl Phys Lett 93:103511
13. Bai X, Wen Y, Yang J, Li P, Qiu J, Zhu Y (2012) A magnetoelectric energy harvester with the magnetic coupling to enhance the output performance. J Appl Phys 111:07A938
14. Srinivasan G, Priya S, Sun N (2015) Composite magnetoelectrics: materials, structures, and applications. Woodhead Publishing, Cambridge
15. Bibes M, Barthelemy A (2008) Multiferroics: towards a magnetoelectric memory. Nat Mater 7:425
16. Hu J, Li Z, Wang J, Nan CW (2010) Electric-field control of strain-mediated magnetoelectric random access memory. J Appl Phys 107:093912
17. Shi Z, Wang C, Liu X, Nan C (2008) A four-state memory cell based on magnetoelectric composite. Chinese Sci Bull 53:2135
18. Fusil S, Garcia V, Barthelemy A, Bibes M (2014) Magnetoelectric devices for spintronics. AnnuRev Mater Res 44:91
19. Gajek M, Bibes M, Fusil S, Bouzehouane K, Fontcuberta J, Barthélémy A, Fert A (2007) Tunnel junctions with multiferroic barriers. Nat Mater 6:296
20. Martin LW, Chu YH, Zhan Q, Ramesh R, Han SJ, Wang SX, Warusawithana M, Schlom DG (2007) Room temperature exchange bias and spin valves based on $BiFeO_3/SrRuO_3/SrTiO_3$/Si (001) heterostructures. Appl Phys Lett 91:172513
21. Ryu J, Carazo AV, Uchino K, Kim HE (2001) Magnetoelectric properties in piezoelectric and magnetostrictive laminate composites. Japan J Appl Phys 40:4948
22. Laletsin U, Padubnaya N, Srinivasan G, DeVreugd CP (2004) Frequency dependence of magnetoelectric interactions in layered structures of ferromagnetic alloys and piezoelectric oxides. Appl Phys A 78:33
23. Han TC, Hsu WL, Lee WD (2011) Grain size-dependent magnetic and electric properties in nanosized $YMnO_3$ multiferroic ceramics. Nanoscale Res Lett 6:201
24. Gerngross MD, Carstensen J, Föll H (2012) Electrochemical and galvanic fabrication of a magnetoelectric composite sensor based on InP. Nanoscale Res Lett 7:379
25. Liu X, Liu S, Han MG, Zhao L, Deng H, Li J, Zhu Y, Krusin-Elbaum L, O'Brien S (2013) Magnetoelectricity in $CoFe_2O_4$ nanocrystal-P(VDF-HFP) thin films. Nanoscale Res Lett 8:374
26. Catalan G, Scott JF (2009) Physics and applications of bismuth ferrite. Adv Mater 21:2463
27. Wang J, Neaton JB, Zheng H, Nagarajan V, Ogale SB, Liu B, Viehland D, Vaithyanathan V, Schlom DG, Waghmare UV, Spaldin NA, Rabe KM, Wuttig M, Ramesh R (2003) Epitaxial $BiFeO_3$ multiferroic thin film heterostructures. Science 299:1719
28. Park T-J, Papaefthymiou GC, Viescas AJ, Lee Y, Zhou H, Wong SS (2010) Composition-dependent magnetic properties of $BiFeO_3$-$BaTiO_3$ solid solution nanostructures. Phys Rev B 82:024431
29. Zhang Y, Zhang H, Yin J, Zhang H, Chen J, Wang W, Wu G (2010) Structural and magnetic properties in $Bi_{1-x}R_xFeO_3$ (x=0-1, R=La, Nd, Sm, Eu and Tb) polycrystalline ceramics. J Magn Magn Mater 322:2251
30. Mathe VL, Patankar KK, Patil RN, Lokhande CD (2004) Synthesis and dielectric properties of $Bi_{1-x}Nd_xFeO_3$ perovskites. J Magn Magn Mater 270:380
31. Lomanova NA, Semenov VG, Panchuk VV, Gusarov VV (2012) Structural changes in the homologous series of the Aurivillius phases $Bi_{n+1}Fe_{n-3}Ti_3O_{3n+3}$. J Alloy Compd 528:103
32. Srinivas A, Suryanarayana SV, Kumar GS, Mahesh Kumar M (1999) Magnetoelectric measurements on $Bi_5FeTi_3O_{15}$ and $Bi_6Fe_2Ti_3O_{18}$. J Phys Condens Mat 11:3335
33. Duong GV, Groessinger R, Schoenhart M, Bueno-Basques D (2007) The lock-in technique for studying magnetoelectric effect. J Magn Magn Mater 316:390
34. Yang SCh, Kumar A, Petkov V, Priya S (2013) Room-temperature magnetoelectric coupling in single-phase $BaTiO_3$-$BiFeO_3$ system. *J Appl Phys 2013*, **113**:144101-1
35. Kowal K, Jartych E, Guzdek P, Lisinska-Czekaj A, Czekaj D (2015) Magnetoelectric effect in $(BiFeO_3)_x$–$(BaTiO_3)_{1-x}$ solid solutions. Mat Sci Pol 33:107
36. Dzik J, Lisinska-Czekaj A, Zarycka A, Czekaj D (2013) Study of phase and chemical composition of $Bi_{1-x}Nd_xFeO_3$ powders derived by pressureless sintering. Arch Metall Mater 58:1371
37. Pikula T, Dzik J, Lisinska-Czekaj A, Czekaj D, Jartych E (2014) Structure and hyperfine interactions in $Bi_{1-x}Nd_xFeO_3$ solid solutions prepared by solid-state sintering. J Alloy Compd 606:1
38. Jartych E, Mazurek M, Lisinska-Czekaj A, Czekaj D (2010) Hyperfine interactions in some Aurivillius $Bi_{m+1}Ti_3Fe_{m-3}O_{3m+3}$ compounds. J Magn Magn Mater 322:51
39. Pikula T, Guzdek P, Dzik J, Lisinska-Czekaj A, Jartych E (2015) X-ray diffraction, Mössbauer spectroscopy, and magnetoelectric effect studies of multiferroic $Bi_5Ti_3FeO_{15}$ ceramics. Acta Phys Pol 127:296
40. Chandarak S, Unruan M, Sareein T, Ngamjarurojana A, Maensiri S, Laoratanakul P, Ananta S, Yimnirun R (2009) Fabrication and characterization of (1–x)$BiFeO_3$-x$BaTiO_3$ ceramics prepared by a solid state reaction method. J Magnetics 14:120
41. Ismailzade IH, Ismailov RM, Alekberov AI, Salaev FM (1981) Investigation of the magnetoelectric (ME)H effect in solid solutions of the systems $BiFeO_3$-$BaTiO_3$ and $BiFeO_3$-$PbTiO_3$. Phys Stat Sol A 68:K81
42. Kowal K, Jartych E, Guzdek P, Stoch P, Wodecka-Dus B, Lisinska-Czekaj A, Czekaj D (2013) X-ray diffraction, Mössbauer spectroscopy, and magnetoelectric effect studies of $(BiFeO_3)_x$-$(BaTiO_3)_{1-x}$ solid solutions. Nukleonika 58:57
43. Malesa B, Antolak-Dudka A, Oleszak D, Pikula T (2015) Structure and Mössbauer spectroscopy studies of mechanically activated $(BiFeO_3)_{1-x}$-$(BaTiO_3)_x$ solid solutions. Nukleonika 60:109
44. Goossenes DJ, Weekes CJ, Avdeev M, Hutchison WD (2013) Crystal and magnetic structure of (1-x)$BiFeO_3$-x$SrTiO_3$ (x=0.2, 0.3, 0.4, and 0.8). J Solid State Chem 207:111
45. Jartych E, Pikula T, Mazurek M, Lisinska-Czekaj A, Czekaj D, Gaska K, Przewoznik J, Kapusta C, Surowiec Z (2013) Antiferromagnetic spin glass-like behavior in sintered multiferroic Aurivillius $Bi_{m+1}Ti_3Fe_{m-3}O_{3m+3}$ compounds. J Magn Magn Mater 342:27
46. Birenbaum AY, Ederer C (2014) Potentially multiferroic Aurivillius phase $Bi_5FeTi_3O_{15}$: cation site preference, electric polarization, and magnetic coupling from first principles. Phys Rev B 90:214109
47. Zhao H, Kimura H, Cheng Z, Osada M, Wang J, Wang X, Dou S, Liu Y, Yu J, Matsumoto T, Tohei T, Shibata N, Ikuhara Y (2014) Large magnetoelectric coupling in magnetically short-range ordered $Bi_5Ti_3FeO_{15}$ film. Sci Rep 4:5255
48. Jartych E, Pikula T, Kowal K, Lisinska-Czekaj A, Czekaj D (2014) Mössbauer spectroscopy and magnetoelectric effect studies of multiferroic ceramics based on $BiFeO_3$. Key Eng Mater 602–603:936